A Distributed, Phase-locked, Class-E, RF Generator with Automatic Zero-Voltage Switching

Robert A. Moffatt[1]*, Trevor Howarth[1], Connor Gafner[1], Jeffrey J. Yen[1], Feng-Kai Chen[1], Joshua Yu[1]
[1]Etherdyne Technologies, Inc., Palo Alto, CA, USA
*ramoffatt@etherdyne.net

***Abstract*—In this paper, a system is described which is capable of driving an RF current in a large, flexible, resonant wire structure using a distributed RF generator, consisting of multiple phase-locked, Class-E RF generators with Automatic Zero-Voltage Switching (AZVS). This distributed RF generator passively maintains a constant RF current amplitude under varying load conditions, without the need for an active impedance-matching network. In addition, the Automatic Zero-Voltage Switching allows efficient Class-E operation over a range of resonant frequencies.**

This wire structure may be cut to length and reshaped to fit areas of different size without the need for adaptive impedance-matching. By enabling large volumes of space to be filled with an oscillating magnetic field, the distributed RF generator described in this paper finds immediate application for the purpose of resonant magnetic wireless power transfer in large spaces.

***Index Terms*—distributed, phase-locked, ZVS, AZVS, Class-E**

I. Introduction

The recent proliferation of small sensors and the Internet-of-Things (IoT) has introduced a new need for powering a large number of small devices within a large, pre-defined area, such as a room, factory, grain silo, etc. Because wires limit device mobility, and batteries place strict limitations on device functionality and lifetime, a wireless power solution is desirable.

The system we describe in this paper delivers wireless power via a resonant near-field magnetic loop antenna, which fills the entire volume of interest with an oscillating magnetic field. In order to simplify installation, it is desirable for the system to be relatively insensitive to both the exact shape and size of the loop antenna, while also maintaining consistent operation under varying load conditions. We describe a distributed RF generator design[2] which can drive a resonant near-field magnetic loop antenna while simultaneously satisfying both of these conditions.

II. A Resonant, Near-Field Magnetic Loop Antenna of Variable Shape and Size

Resonant wireless power utilizes resonant dipole receivers which absorb power from an oscillating ambient field. In general, both the dipoles and the ambient field may be electric, magnetic, or some combination thereof. For our purposes, we chose to utilize magnetic dipoles and magnetic fields due to their weaker interaction with the human body. The 6.78MHz ISM frequency was chosen as the frequency of operation due to its long wavelength, which helps to suppresses unwanted far-field radiation.

To generate the oscillating ambient magnetic field, we utilize a near-field resonant magnetic loop antenna which encloses the area within which the receiver devices are to be placed. The loop dimensions are assumed to be sub-wavelength, ensuring that receivers in the vicinity of the loop are always within the near field.

It is desirable for the resonant magnetic loop antenna to be capable of assuming many different shapes and sizes in order to fit the dimensions of the area to be powered. Figure 1 illustrates a simple example of how this can be accomplished. The figure depicts a square loop of width, w, composed of wire segments of length, s, joined by capacitors of capacitance, C. Assuming the wire has a circular cross-section with radius, a, the inductance per unit length of wire, l is given by: [1]

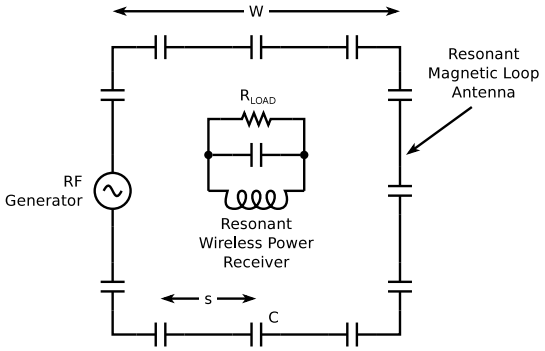

Fig. 1. A square magnetic loop antenna of width, w, composed of wire with circular cross-section of radius, a. The wire is divided into segments of length, s, joined by capacitors of capacitance, C. If C, s, and a are held fixed, it is found that the resonant frequency of this loop depends only weakly on the width, w. It is assumed that the width of the loop is small relative to the wavelength.

$$l = \frac{L_0}{4w} = \frac{\mu}{2\pi}\left(\ln\left(\frac{w}{a}\right) - 0.77401\ldots\right) \tag{1}$$

where L_0 is the inductance of the loop, and μ is the permeability of the surrounding medium. The number of capacitors, N, is given by the total perimeter divided by the segment length:

$$N = \frac{4w}{s} \tag{2}$$

[2]Patent pending.

The resonant frequency, f_0, of the distributed-capacitor loop is given by:

$$f_0 = \frac{1}{2\pi\sqrt{L_0 C_0}} = \frac{1}{2\pi\sqrt{lsC}} \tag{3}$$

where $C_0 = C/N = s\,C/(4w)$ is the total series capacitance of the loop. It can be seen from Equations 3 and 1 that the resonant frequency of the loop depends strongly on the segment length, s, and the capacitance, C, but only weakly (i.e. logarithmically) on the size of the loop, w, and the wire radius, a. Therefore, if C, s, and a remain fixed, the resonant frequency of the loop is substantially independent of its size. For example, if the loop is composed of 14 gauge wire (0.81mm radius), the resonant frequency will vary by less than 5% if the width is doubled from 5 meters to 10 meters.

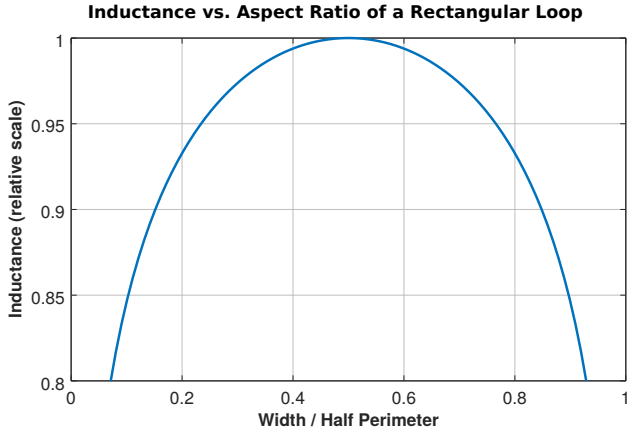

Fig. 2. Theoretical inductance of a rectangular loop relative to the inductance of a square loop of equal perimeter. The loop is assumed to be made from 14 gauge wire, with a perimeter of 212in (5.38m), which matches the wire radius and perimeter of the loop shown in Figure 10.

It is desirable that the resonant frequency be substantially independent not only of the size of the loop, but also of its shape. Figure 2 illustrates that this is indeed the case for a rectangular loop, since the inductance per unit length is seen to vary by no more than 5% as the aspect ratio is varied from 1:1 to 3:1, which corresponds to a 2.4% variation in resonant frequency.

For a loop of wire in the shape of a general planar curve, the inductance per unit length, l, is approximated by: [1]

$$l = \frac{\mu}{2\pi}\left(\ln\left(\frac{2\mathcal{S}}{a}\right) + \ln\left(\frac{\mathcal{A}}{\mathcal{S}^2}\right) - 0.0809\ldots\right) \tag{4}$$

where $\mathcal{S}$ is the total length of the wire, $\mathcal{A}$ is its enclosed area, and a is the wire radius. It can be seen from Equation 4 that l varies only weakly (i.e. logarithmically) with the length or area of the curve. Therefore, as long as the RF generator is capable of driving a resonant load over a relatively small range of resonant frequencies (e.g. $\pm 5\%$), it will be capable of driving distributed-capacitor loops spanning a very practical range of geometries.

III. A Class-E Amplifier with Automatic Zero-Voltage Switching

A commonly-used amplifier for driving a series-resonant near-field magnetic loop antenna is the Class-E amplifier shown in Figure 3. [2] [3] Because the MOSFET, Q_1, is driven in switching mode, this amplifier topology is very well-suited for the purpose of generating an unmodulated RF sine wave with very high DC-to-RF conversion efficiency.

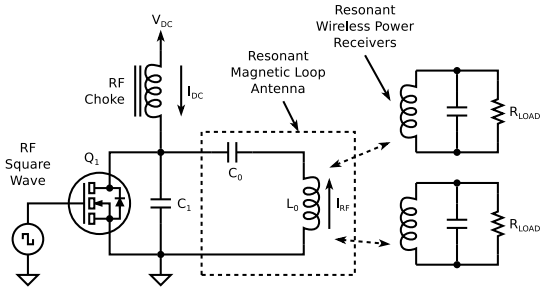

Fig. 3. A basic, Class-E amplifier, driving a resonant magnetic loop antenna, represented by the lumped-element equivalent circuit components C_0 and L_0. The current, I_{RF}, generates the oscillating magnetic field which delivers power to the loads, which are represented by resistors connected to resonant magnetic dipole receivers.

However, in order to achieve high efficiency, it is essential that the drain voltage of the MOSFET, Q_1, be zero at the instant when Q_1 turns on, a condition known as Zero-Voltage Switching (ZVS). Otherwise, the capacitor, C_1, will discharge through Q_1, dumping its stored energy into heat once per cycle. The zero-crossing-time of the drain waveform will vary depending on the tuning and load conditions of the loop. Consequently, the amplifier shown in Figure 3 tends to be efficient for only a very narrow range of conditions.

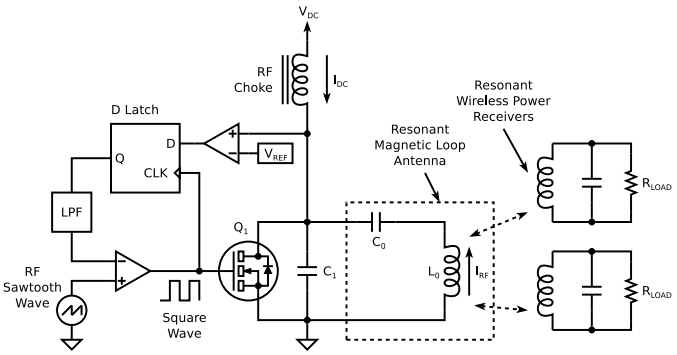

Fig. 4. A Class-E amplifier, with Automatic Zero-Voltage Switching (AZVS). The reference voltage, V_{REF}, is set to be as close to 0V as possible, while still being larger than the amplitude of any drain voltage ringing caused by parasitic inductance. The feedback network varies the duty cycle of the gate drive to ensure that the ZVS condition is always met.

This problem may be solved using Automatic Zero-Voltage Switching (AZVS), as shown in Figure 4. A comparator and latch detect whether the drain voltage of Q_1 is above or below a reference voltage, V_{REF}, at the instant when Q_1 turns on. The output of the latch is low-pass-filtered and used as a feedback

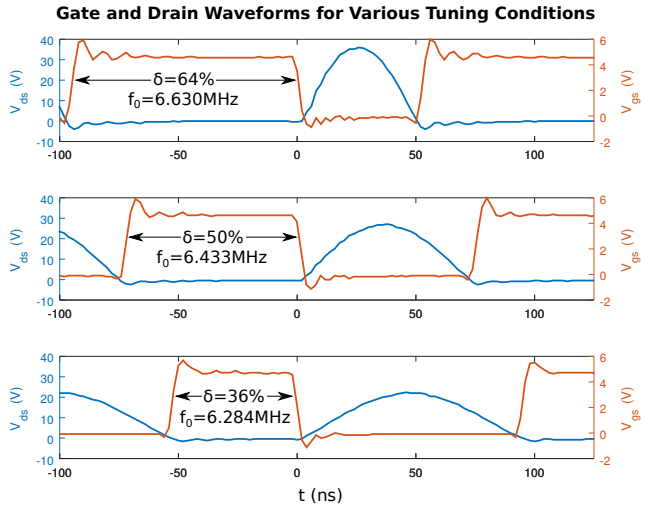

Fig. 5. Measured gate and drain voltage waveforms for a Class-E amplifier with Automatic Zero-Voltage Switching (AZVS) for various tuning conditions, and for $K = 0.2$, $f_d = 6.780$MHz, $V_{DC} = 8.0V$, and $C_1 = 1$nF. The AZVS feedback circuitry automatically ensures that the ZVS condition is always met. Note that the amplitude of the drain voltage waveform varies with the tuning condition.

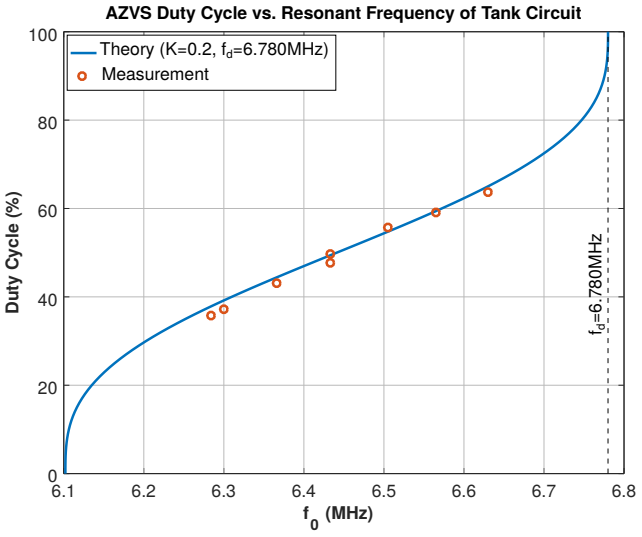

Fig. 6. Red dots show the measured duty cycle of the AZVS amplifier as a function of the resonant frequency, f_0, of the tank circuit. The resonant frequency of the tank circuit was changed by changing the shape of the loop. The blue curve shows the theoretical relation between the resonant frequency and the duty cycle given by Equation 5.

signal to control the duty cycle of the gate drive waveform. The feedback shifts the time at which Q_1 turns on until the drain voltage of Q_1 is equal to V_{REF} at the the rising edge of the gate drive signal. If V_{REF} is very close to zero, then this feedback loop automatically maintains the amplifier in a state of ZVS operation.

Figure 5 shows measurements of the gate and drain waveforms of a Class-E amplifier with AZVS for three different

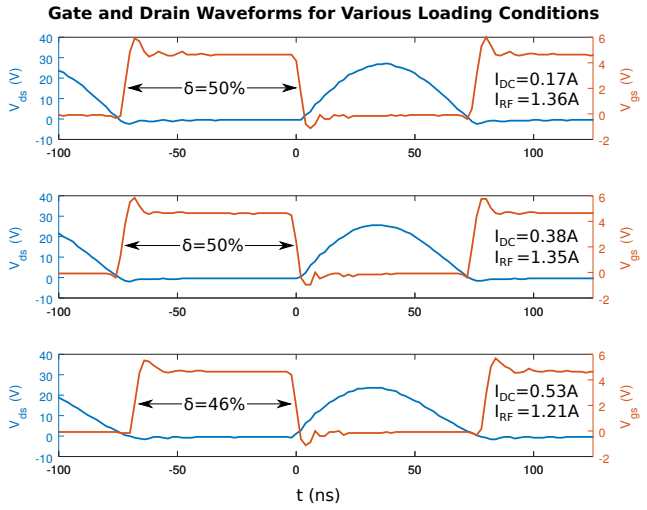

Fig. 7. Measured gate and drain voltage waveforms for a Class-E amplifier with Automatic Zero-Voltage Switching (AZVS) for various loading conditions, and for $K = 0.2$, $f_d = 6.780$MHz, $V_{DC} = 8.0V$, and $C_1 = 1$nF. The AZVS feedback circuitry automatically ensures that the ZVS condition is always met. Note that the RF current amplitude is is relatively constant over a wide range of loading conditions.

tuning conditions. The measured waveforms show that the AZVS feedback circuit adjusts the rising edge of the gate drive signal to always be synchronous with the zero-crossing of the drain waveform, even as the detuning causes this zero-crossing to shift earlier or later in the cycle.

For a given drive frequency, f_d, and a given resonant frequency of the loop antenna tank circuit, f_0, there will be a certain gate-drive duty cycle, δ, at which the ZVS condition is met. The relation between δ, f_0, and f_d is approximately given by:

$$\frac{f_0}{f_d} \approx 1 - \frac{K}{2}\left(1 - \delta + \frac{\sin(2\pi\delta)}{2\pi}\right) \tag{5}$$

where the dimensionless constant, K, is defined as:

$$K \equiv \frac{C_0}{C_0 + C_1} = \frac{\chi_1}{\chi_1 + \chi_0} \tag{6}$$

and where $\chi_0 = 1/(2\pi f_d C_0)$ and $\chi_1 = 1/(2\pi f_d C_1)$ are the reactances of C_0 and C_1 respectively. Equation 5 is a valid approximation when $K \ll 1$ and under light loading conditions, defined as $I_{DC} \ll I_{RF}$, where I_{DC} and I_{RF} are the DC and RF currents of the Class-E amplifier (see Figure 4).

Because the duty cycle must be between 0 and 1, the resonant frequency of the loop must satisfy the following constraint in order for the feedback loop to be capable of finding a ZVS operating point:

$$1 - \frac{K}{2} < \frac{f_0}{f_d} < 1 \tag{7}$$

Therefore, the relation between the tuning range, Δf_0, and the constant, K, is given by:

$$K > 2\frac{\Delta f_0}{f_d} \tag{8}$$

Figure 6 shows experimental measurements (red dots) of the duty cycle as a function of the resonant frequency of the tank circuit for a Class-E amplifier with AZVS, and with $K = 0.2$ and $f_{\mathrm{d}} = 6.780$MHz. The data are found to be in close agreement with the theoretical relation (blue curve) given by Equation 5.

Because the peak drain voltage and RF current amplitude vary with duty cycle (see Figure 5), it is desirable to keep the duty cycle within certain pre-defined limits to prevent these voltages and currents from approaching extreme values. In the circuit which was used to produce the data in this section, the duty cycle was constrained to be between 36% and 64%.[3] This limited the tuning range, Δf_0, to be approximately half of the upper bound given by Condition 8, giving a fractional tuning range of $\Delta f_0 / f_{\mathrm{d}} = 5\%$.[4]

The tuning of the loop is primarily determined by its geometry, which typically does not change after installation. However, in most applications, the number and placement of the loads may vary in the course of normal use. It is therefore important to know how the system will respond to variations in the loading condition. Figure 7 shows experimental measurements of the RF current amplitude as a function of the loading condition of the loop. As resonant wireless receivers were moved closer and farther from the loop, the DC current drawn by the Class-E amplifier varied by over a factor of three. However, the RF current amplitude varied by only about 12% in the most extreme case. In addition, the amplifier maintained the ZVS operating condition over the entire range of loading conditions. This indicates that the RF current amplitude and the amplifier efficiency are both relatively insensitive to the loading conditions of the loop.

IV. Series Distributed RF Generators

The AZVS amplifier described in the previous section allows efficient operation to be maintained under varying load conditions, and in the presence of detuning due to variations in the shape of the loop. However, another problem arises for loops of varying size. As the size of the loop grows, its inductance increases. The total series capacitance, C_0, must therefore decrease. If the capacitor, C_1, remains fixed, then according to Equation 6, K must decrease. Eventually, there will come a point where Condition 8 is no longer satisfied, and the AZVS amplifier will no longer be capable of accommodating the desired tuning range, Δf_0.

It is possible to reduce C_1 with increasing loop size, but that is undesirable two reasons. First, in order for the RF current amplitude to be held constant, the DC supply voltage would need to vary inversely with C_1, requiring the use of components with a very high voltage rating as the loop size becomes large. Second, if the loop is driven from one point, the RF input impedance at the drive point grows continually larger as the size of the loop grows. A high impedance at the drive point means that a high RF voltage and high electric field will be present at that point and in its vicinity. This electric field has the potential not only to cause losses in nearby dielectrics, but also safety concerns due to the possible absorption of RF power in human tissue via stray electric fields.

Both of these problems are solved by driving the loop from multiple points with multiple, synchronized RF generators. Each RF generator requires a source of DC power. While it is possible to run a separate power cable to each generator, this would vastly increase the amount of wiring. It is therefore desirable to power the generators without any additional wiring other than the wire of the loop itself.

This is achieved by adding RF chokes in parallel with the distributed capacitors of the loop, which allow the loop to support both a DC and an RF current simultaneously. Each RF generator takes in DC power and outputs RF power through the same two terminals. Figure 8 shows how the Class-E amplifier from Figure 4 is modified in order to accomplish this.

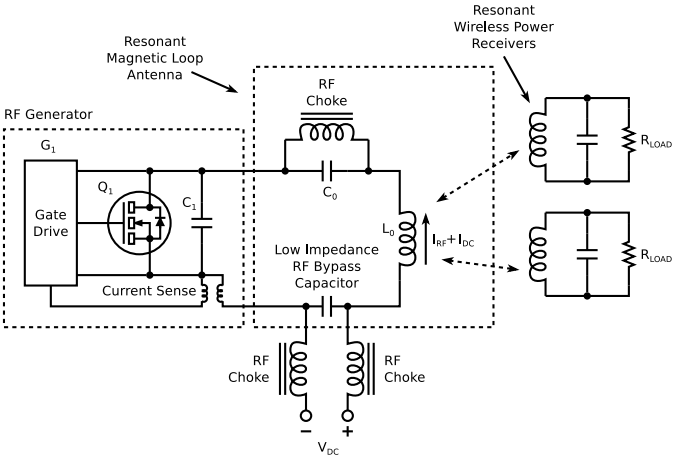

Fig. 8. A Class-E amplifier, rearranged so that the RF generator draws its DC power from the same two terminals it uses to output RF power. The gate drive circuit, G_1, uses the drain-to-source voltage of Q_1 as a source of power in addition to using it as an input signal to the AZVS feedback loop. G_1 also contains an additional input connected to a current-sensing transformer, which is used to lock the phase of an internal oscillator to the phase of the RF current circulating around the loop. This phase-locking is necessary to lock the phases of multiple RF generators when they are connected together in series.

Figure 9 shows how multiple RF generators, like the one in Figure 8, may be connected in series and distributed around the loop. In general, the loop consists of N_{a} active RF generators, and N_{p} passive joints, connected by lengths of wire. Each passive joint consists of a capacitor in parallel with an RF choke. The RF chokes are chosen to have a high impedance at the drive frequency so as to not significantly affect the resonance of the loop, but still allow DC current to flow around the loop.

[3]Other choices are possible. Kazimierczuk and Puczko, for example, recommend lower and upper limits of 25% and 75%, respectively. [2]

[4]Note that the drive frequency, f_{d}, was held fixed while the resonant frequency of the tank circuit, f_0, was varied. In other applications, it may be more natural to hold f_0 fixed while varying f_{d}. In that case, Condition 7 can be rearranged to give an upper limit on the drive frequency range, Δf_{d}, of the amplifier:

$$\frac{\Delta f_{\mathrm{d}}}{f_0} < \frac{K}{2-K} \approx \frac{K}{2} \tag{9}$$

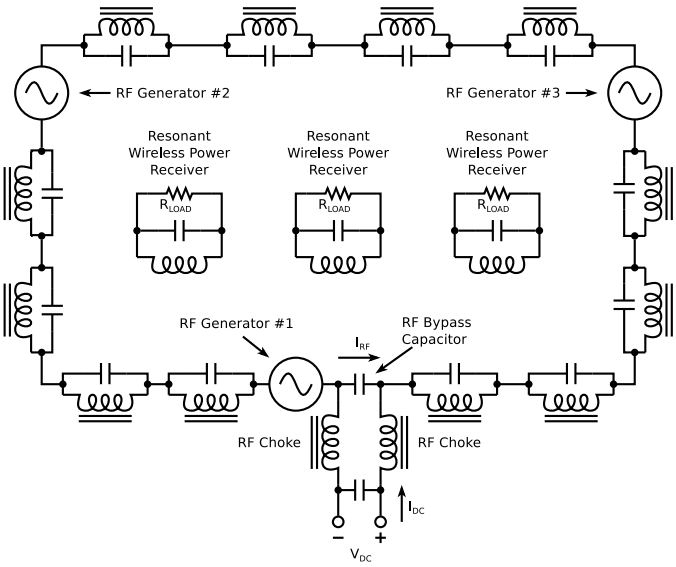

Fig. 9. Simplified schematic of a resonant magnetic loop antenna driven by distributed RF generators. The RF generators use the same two terminals as both a DC power input and an RF power output. Figure 10 shows a photograph of the physical embodiment of this system.

For the distributed version of the Class-E amplifier, the value of the constant, K, is given by:

$$K = \frac{\chi_1}{\chi_1 + \chi_0} = \frac{1}{1 + \frac{\chi_0}{\chi_1}} = \frac{1}{1 + \frac{N_\mathrm{p}\chi_0^{(\mathrm{sing.})}}{N_\mathrm{a}\chi_1^{(\mathrm{sing.})}}} \tag{10}$$

where χ_0 is the total series reactance of all of the passive joints, χ_1 is the total series reactance of all of the capacitors of the active joints, $\chi_0^{(\mathrm{sing.})}$ is the reactance of a single passive joint, and $\chi_1^{(\mathrm{sing.})}$ is the reactance of the capacitor of a single active joint. If the ratio, $(N_\mathrm{p}\chi_0^{(\mathrm{sing.})})/(N_\mathrm{a}\chi_1^{(\mathrm{sing.})})$, is held fixed, then Equation 10 implies that K is independent of the size of the loop. Therefore, unlike the case of a loop containing a single RF generator and single drive point, the distributed RF generator can accommodate a tuning range which is independent of the size of the loop without any changes to component values.

V. Phase-Locking

In order to properly drive the loop, all of the distributed RF generators depicted in Figure 9 must be synchronized. While this may be achieved by connecting all of the amplifiers to a common local oscillator via a star configuration, this solution is undesirable, since it would require a separate cable for each RF generator, vastly increasing the amount of wiring. It is therefore desirable to arrange the RF generators so that they lock in phase with each other without any additional wiring other than the wire of the loop itself.

Phase-locking may be achieved by locking each RF generator to the phase of some RF signal which they all share in common. Because all of the RF generators are connected in series, the common RF current shared by all of the RF generators suggests itself as a natural choice for this common signal.

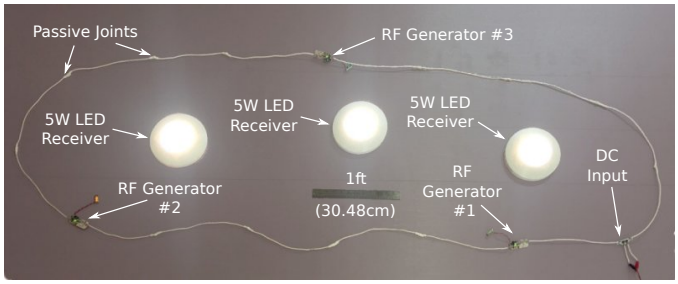

Fig. 10. Photograph of a distributed RF generator powering three wireless receivers. Each receiver delivers a regulated 5W of power to an LED load. The DC input power was 34W (0.6A at 57V). The DC-to-DC efficiency was 44% when the loads were present. The system drew 13W of DC power when the loads were absent.

Figure 8 shows how this phase-locking is accomplished. A current-sensing transformer picks up an induced voltage proportional to the RF current flowing around the loop. The phase of an internal oscillator circuit is then locked to the phase of this induced voltage. The phase-locked oscillator is used to generate the gate-drive waveform. Assuming that all of the RF generators are identical, this guarantees that the gate-drive waveform of each RF generator has the same phase relative to the phase of the RF current, which ensures that all of the RF generators are in phase with respect to each other.

Figure 10 shows a photograph of a wireless power system consisting of a loop with three RF generators and coupled to three regulated wireless loads with an overall DC-to-DC efficiency of 44%. The DC voltages measured across the RF generators were all within about $\pm 10\%$ of the average voltage, which provides an indirect indication of good phase synchronicity.

VI. Conclusion

The distributed RF generator described in this paper enables wireless power to be delivered to devices within a large area by means of a magnetic field generated by a near-field, resonant magnetic loop antenna which may adapted to fit the dimensions of the region to be powered. The Automatic Zero-Voltage Switching (AZVS) of the RF generators allows the loop to assume various shapes, and to power varying numbers of loads, while still maintaining efficient operation. In addition, the distributed nature of the series capacitors and RF generators allows the loop to assume a range of different sizes without requiring adaptive matching. In addition, the DC power delivery and phase-locking of the RF generators is accomplished without the need for any additional wiring other than the wire of the loop itself. Taken together, these features greatly simplify the process of adapting the loop to fit a wide and practically-useful range of geometries.

References

[1] Frederick W. Grover, *Inductance Calculations*. Mineola, New York: Dover Publications, Inc., 1946.

[2] M. Kazimierczuk and K. Puczko, "Exact analysis of class E tuned power amplifier at any Q and switch duty cycle," *IEEE Transactions on Circuits and Systems*, vol. 34, no. 2, pp. 149-159, February 1987.

[3] Michael A. de Rooij, *Wireless Power Handbook*. El Segundo: Power Conversion Publications, 2015.